

Supporting Information

Development of AIEE Active Fluorescent and Colorimetric Probe for Solid, Solution, and Vapor Phase Detection of Cyanide: Smartphone and Food Applications

Shumaila Majeed^a, Muhammad Tahir Waseem^a, Gul Shahzada Khan^b, Hafiz Muhammad Junaid^a, Muhammad Imran^c, Shamyla Nawazish^d, Tausif Ahmad Khan^a, Tariq Mahmood^a, Sohail Anjum Shahzad^{a,*}

^a Department of Chemistry, COMSATS University Islamabad, Abbottabad Campus, University Road, Abbottabad 22060, Pakistan

^b Department of Chemistry, College of Science, University of Bahrain, Sakhir 32038, Bahrain

^c Department of Chemistry, Faculty of Science, King Khalid University, P.O. Box 9004, Abha 61413, Saudi Arabia

^d Department of Environmental Sciences, COMSATS University Islamabad, Abbottabad Campus, Abbottabad 22060, Pakistan

* Corresponding Author: Department of Chemistry, COMSATS University Islamabad, Abbottabad Campus, University Road, Abbottabad 22060, Pakistan (S.A. Shahzad). E-mail address: sashahzad@cuiatd.edu.pk (S.A. Shahzad).

TABLE OF CONTENTS

SI-1. Instruments and reagents-----	S2
Fig. S1. The fluorescence spectral changes of probe 2 at various DMF/H ₂ O ratios and plausible AIEE mechanism-----	S3
Fig. S2. Theoretical representation of the benzenoid and quinonoid form of probe 2 accomplished through Gaussian 09 package at B3LYP/6-31G-----	S3
Fig. S3. The fluorescence spectral changes of probe 2 at various DMF/ethylene glycol ratios----	S4
Fig. S4. The fluorescence spectral changes of probe 2 at its various concentrations-----	S4
Fig. S5. The UV-vis spectral change of probe 2 in the presence of different anions-----	S5
Fig. S6. The fluorescence spectral change of probe 2 in the presence of different anions-----	S5

Fig. S7. The fluorescence change of probe 2 containing CN ⁻ ions in the presence of interferences-----	S6
Table S1. The comparison of LOD for CN ⁻ and other features of probe 2 with already reported CN ⁻ probes-----	S6
Fig. S8. The Benesi–Hildebrand plot of probe 2 between fluorescence response vs increasing concentrations of CN ⁻ -----	S7
Fig. S9. The switchable fluorescence and colorimetric response of probe 2 -----	S8
Fig. S10. The putative sensing mechanism and ¹ H NMR titration of probe 2 upon addition of increasing amounts of CN ⁻ -----	S9
Fig. S11. Frontier molecular orbital (FMO) plots of probe 2 and its probe–CN ⁻ complex-----	S10
Fig. S12. Effect of pH on the enhanced fluorescence emission response of probe 2 towards CN ⁻ -----	S10
Fig. S13. Photostability analysis of probe 2 and 2 –CN ⁻ complex-----	S10
Fig. S14. The fluorescence spectra changes of probe 2 towards endogenous cyanide in food samples-----	S11
Fig. S15. The fluorescence spectra changes of probe 2 towards CN ⁻ spiked industrial wastewater-----	S12
SI-1. NMR spectra of synthesized compounds-----	S13

SI-1. Instruments and reagents

Proton nuclear magnetic resonance (¹H NMR) spectra of compounds **1** and **2** were recorded at Bruker Avance 400 and 500 MHz while ¹³C NMR spectra were carried out at Bruker Avance 100 and 125 MHz. Photophysical properties and sensing studies of compound **2** were scanned through fluorescence spectroscopy (FluoroMax-Plus-P-C, Horiba Jobin Yvon Technology, USA). UV-Vis spectrophotometer (SPECORD 200 PLUS-223E2003C, Analytik Jena, Germany) was used to record absorption spectra. Used reagents and chemicals were acquired from Daejung Chemicals & Metals (Korea), Alfa Aesar (UK), and Sigma Aldrich (USA). The chemicals enlist 9*H*-fluorenone, aniline, 9,9-Bis(4-aminophenyl)fluorene, methanesulfonic acid, ethyl acetate, *n*-hexane, DMSO-*d*₆, salicylaldehyde, methanol, DMF, acetonitrile, THF, DCM, CHCl₃, DMSO, CN⁻, I⁻, NO₃⁻, Cl⁻, F⁻, N₃⁻, Br⁻, H₂PO₄⁻, ClO₄⁻, CH₃COO⁻, and NO₂⁻.

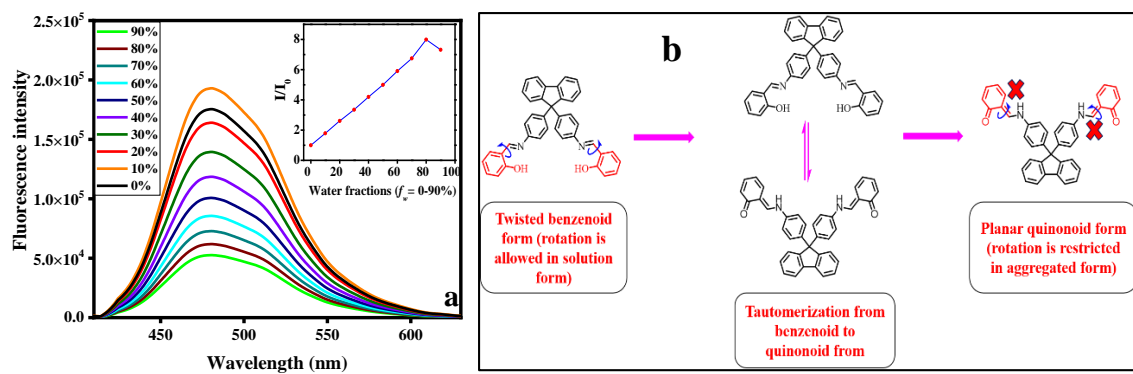


Fig. S1. The fluorescence spectral changes of probe **2** (10 μM) at various DMF/H₂O ratios (a) and plausible AIEE mechanism (b). Inset shows the general representation of AIEE pattern.

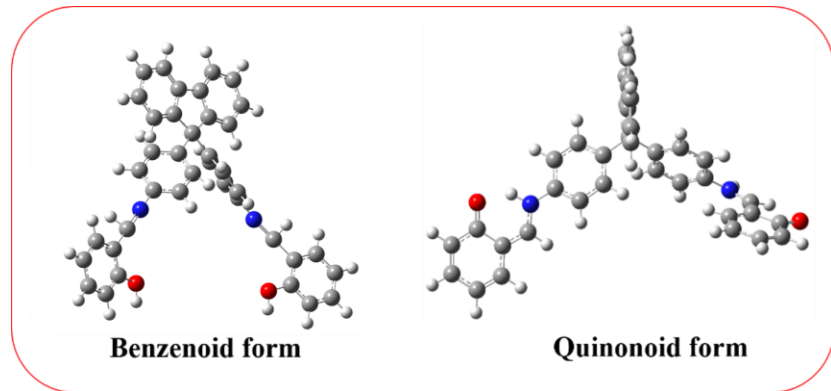


Fig. S2. Theoretical representation of the benzenoid and quinonoid form of probe **2** accomplished through Gaussian 09 package at B3LYP/6-31G (d).

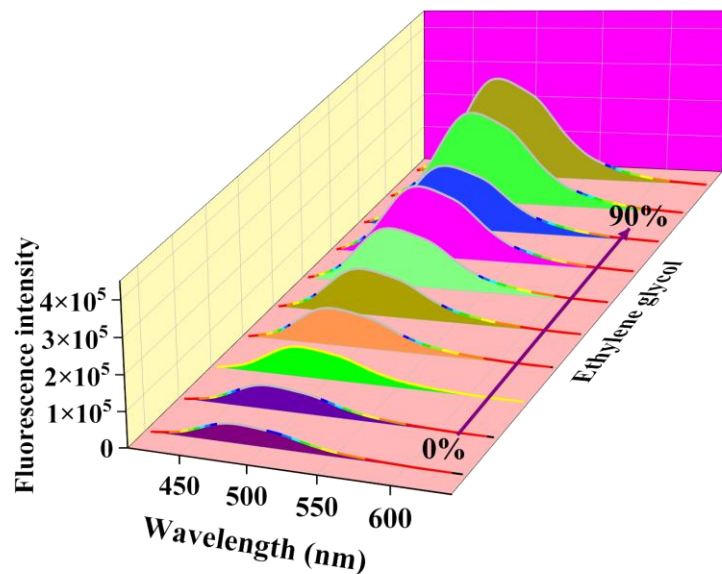


Fig. S3. The fluorescence spectral changes of probe **2** (10 μM) at various DMF/ethylene glycol ratios.

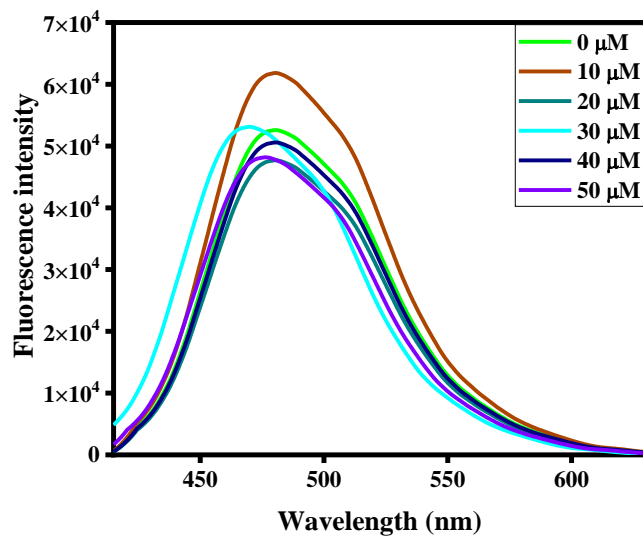


Fig. S4. The fluorescence spectral changes of probe **2** at its various concentrations (0–50 μM).

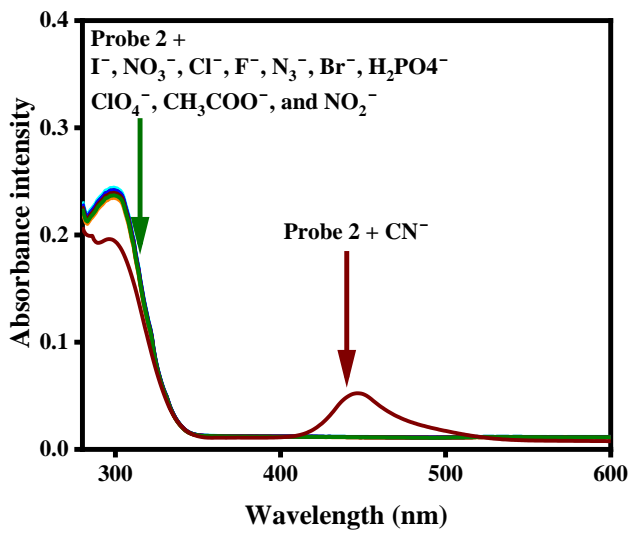


Fig. S5. The UV-vis spectral change of probe **2** (10 μM) in the presence of different anions.

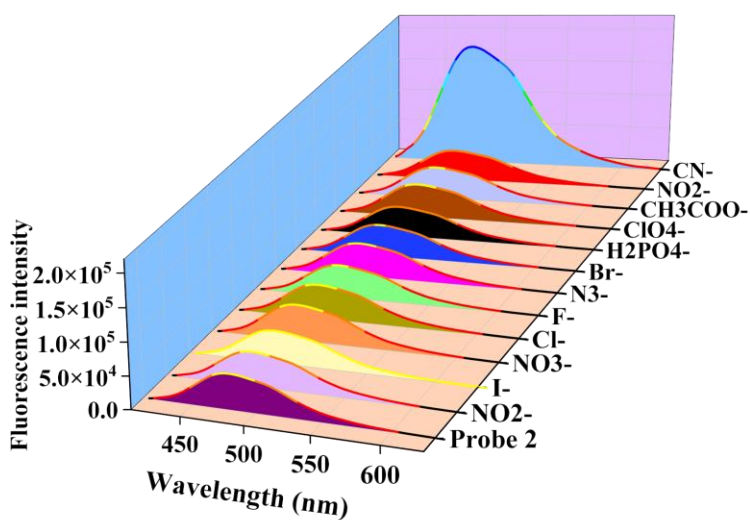


Fig. S6. The fluorescence spectral change of probe **2** (10 μM) in the presence of different anions (Excitation wavelength = 410 nm).

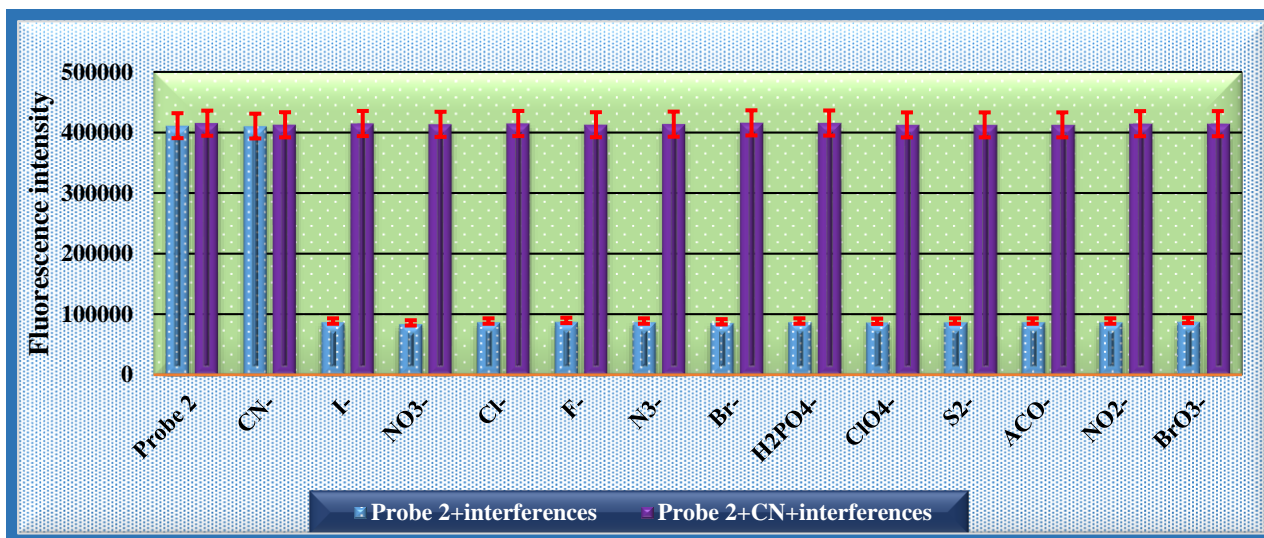


Fig. S7. The fluorescence change of probe **2** (10 μM) containing 50 nM of CN^- ions in the presence of interferences (100 equiv).

Table S1. The comparison of LOD for CN^- and other features of probe **2** with already reported CN^- probes.

Sensors	Aggregation induced emission enhancement (AIEE)	Piezofluorochromic behavior	Vapor phase detection	Detection in actual food Samples	Smartphone based detection	LOD (nM)	Ref.

Schiff base based probe 2	Described in detail	Excellent piezofluorochromic character	Yes	Yes	Yes	6.17	This work
Spiropyran and spironaphthoxazine based sensor	Didn't display	Didn't display	Not described	Not described	Not described	91	1
Naphthopyran benzothiazole core sensor	Didn't display	Didn't display	Not described	Not described	Not described	330	2
aldehyde-appended salamo-type sensor	Didn't display	Didn't display	Not described	Not described	Not described	80	3
Indoleoxazine functionalized compound	Didn't display	Didn't display	Not described	Explored	Not described	100	4
D-π-A organic fluorophore	Didn't display	Didn't display	Not described	Not described	Not described	380	5
Pyridine based nanoparticles as cyanide ion sensor	Explored	Didn't display	Not described	Not described	Not described	8.2	6
Naphthopyran functionalized sensor	Explored	Didn't display	Not described	Not described	Not described	427	7
Oligothiophene-benzothiazole based sensor	Didn't display	Didn't display	Not described	Explored	Not described	15×10^3	8
Triphenylamine based probe	Explored	Didn't display	Not described	Explored	Not described	2×10^4	9
Carbazole based sensor	Explored	Didn't display	Not described	Not described	Not described	67.4	10

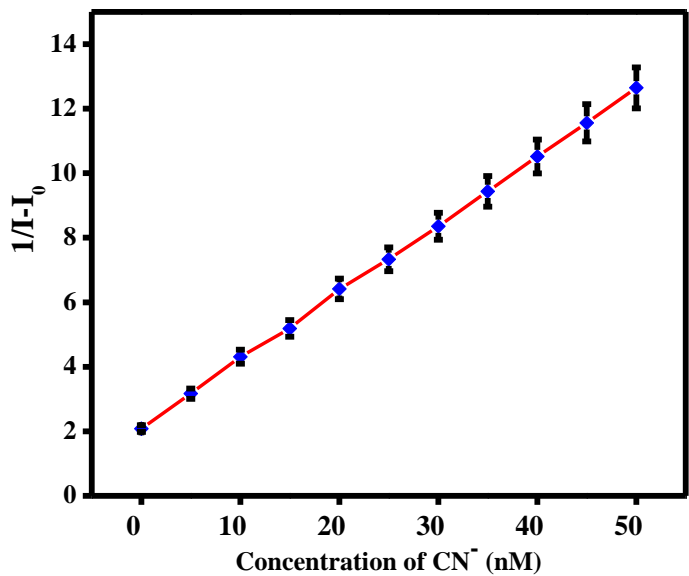


Fig. S8. The Benesi–Hildebrand plot of probe **2** (10 μM) between fluorescence response vs increasing concentrations of CN^- .

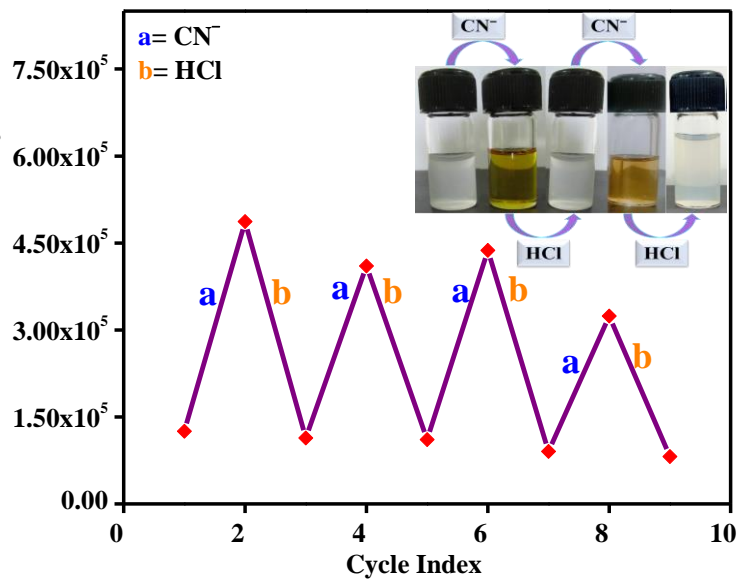


Fig. S9. The switchable fluorescence and colorimetric response of probe **2**.

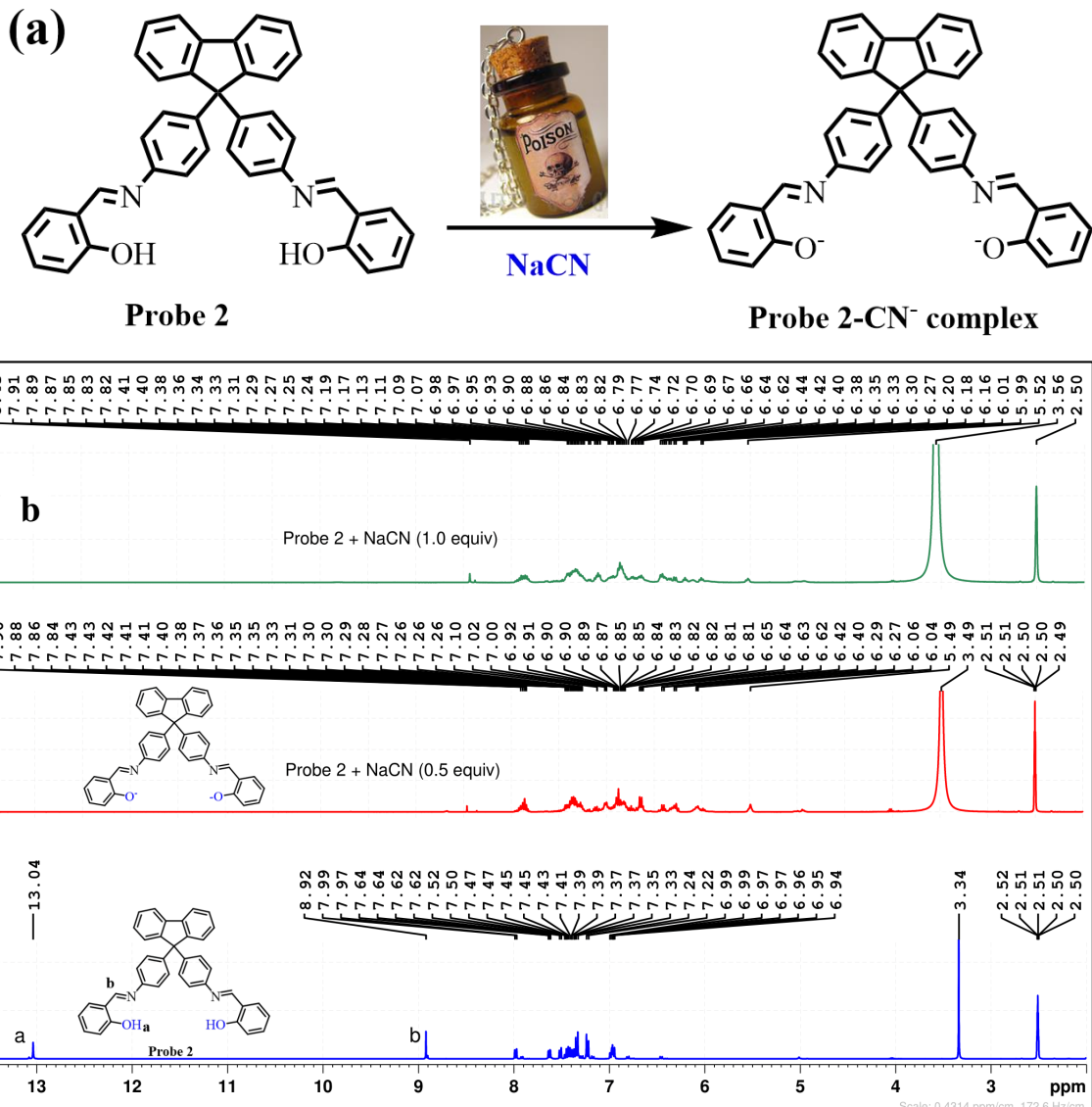


Fig. S10. The putative sensing mechanism (a) and ^1H NMR titration of probe **2** (b) upon addition of increasing amounts of CN^- .

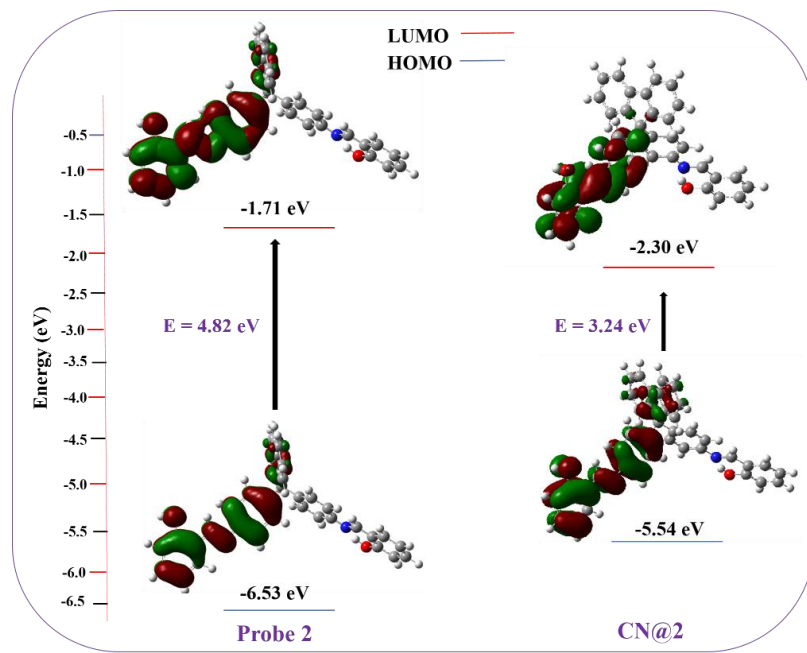


Fig. S11. Frontier molecular orbital (FMO) plots of probe **2** and its probe– CN^- complex (achieved through Gaussian 09 program).

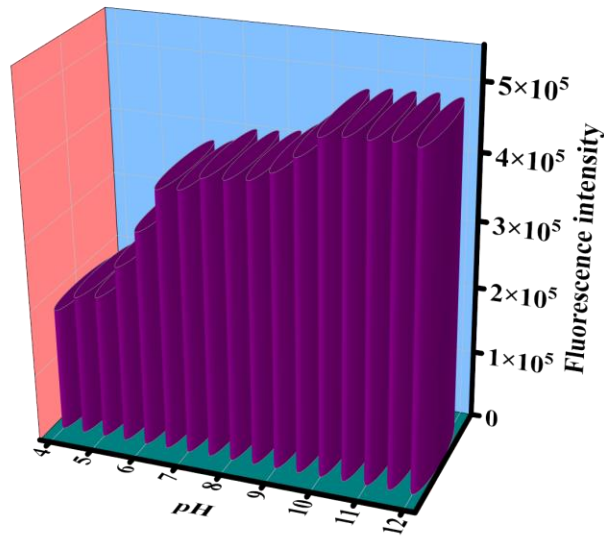


Fig. S12. Effect of pH on the enhanced fluorescence emission response of probe **2** towards CN^- .

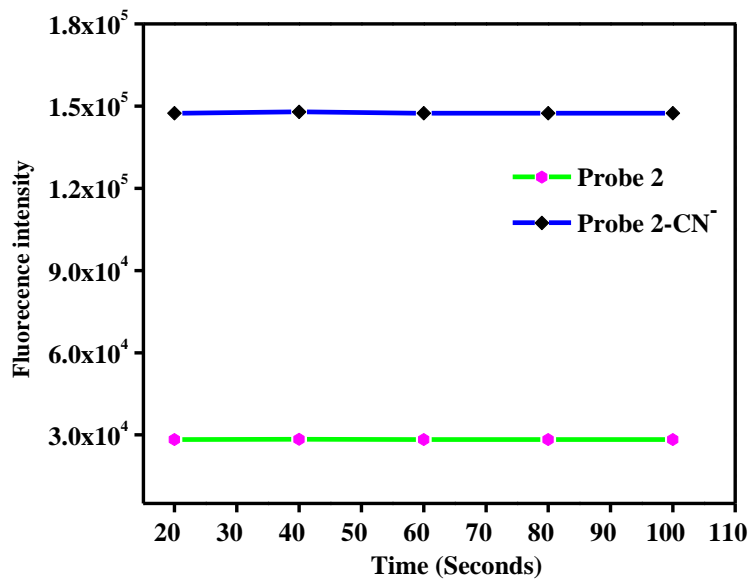
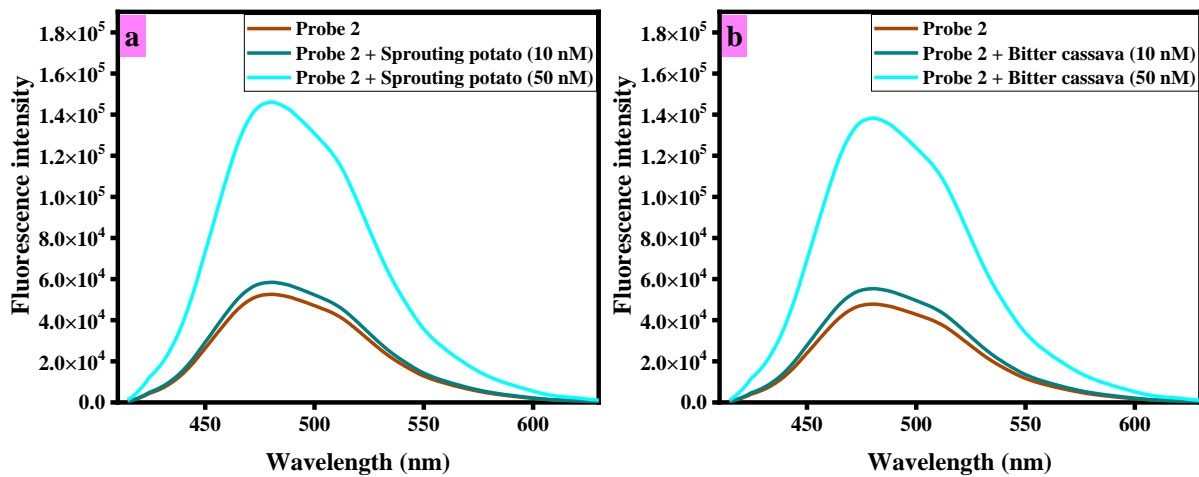


Fig. S13. Photostability analysis of probe **2** and **2**- CN^- complex.



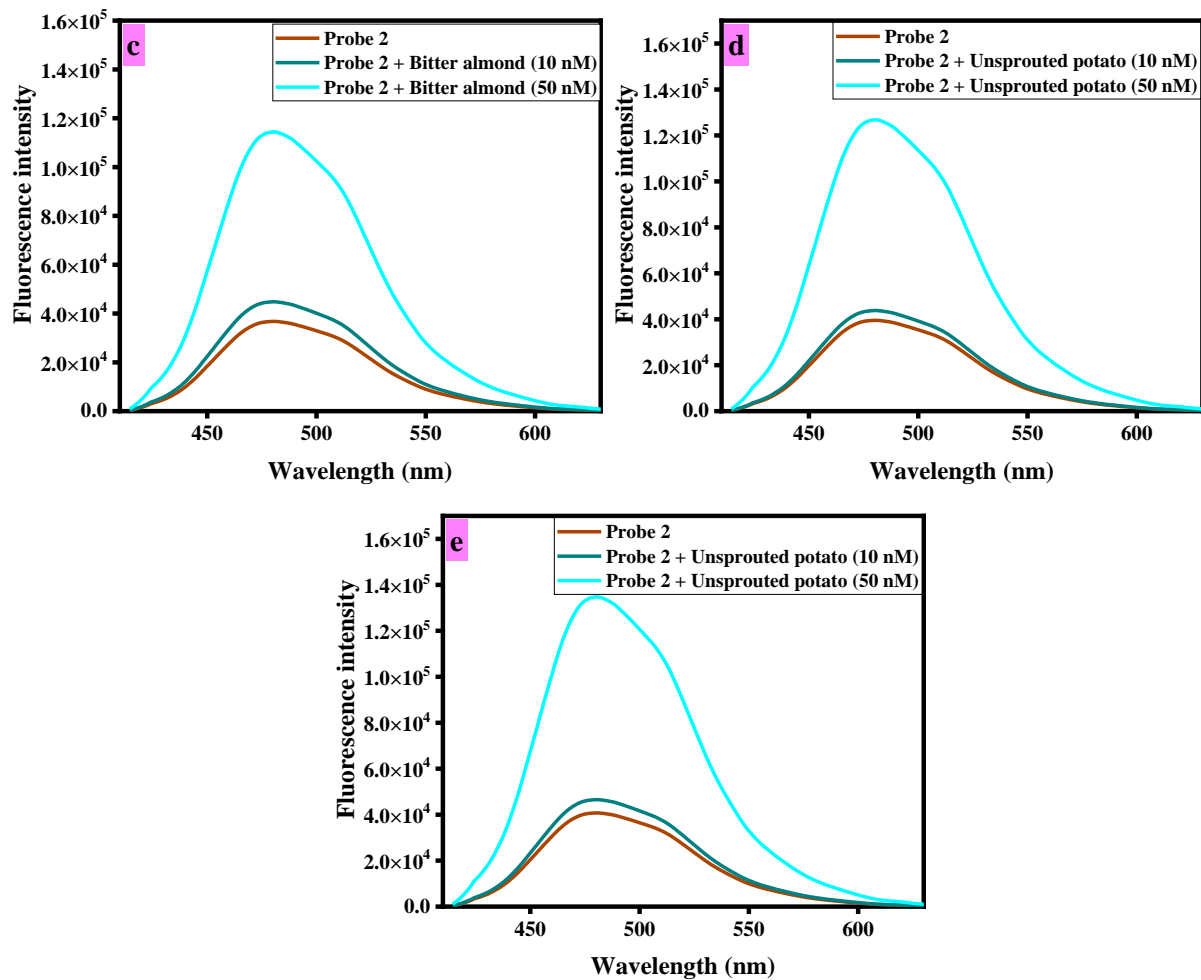


Fig. S14. The fluorescence spectral changes of probe 2 ($10 \mu\text{M}$) towards endogenous cyanide in food samples (sprouting potato (a), bitter cassava (b), bitter almond (c), un-sprouted potatoes (d), and sweet almond (e)).

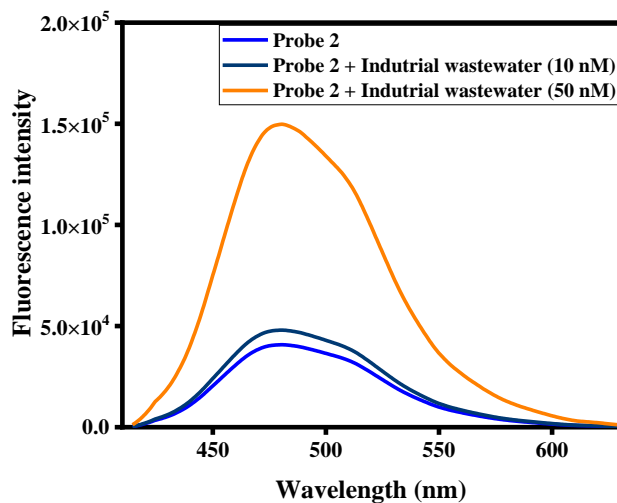
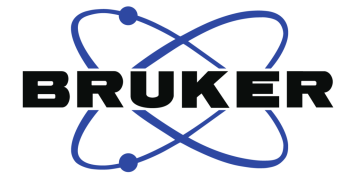
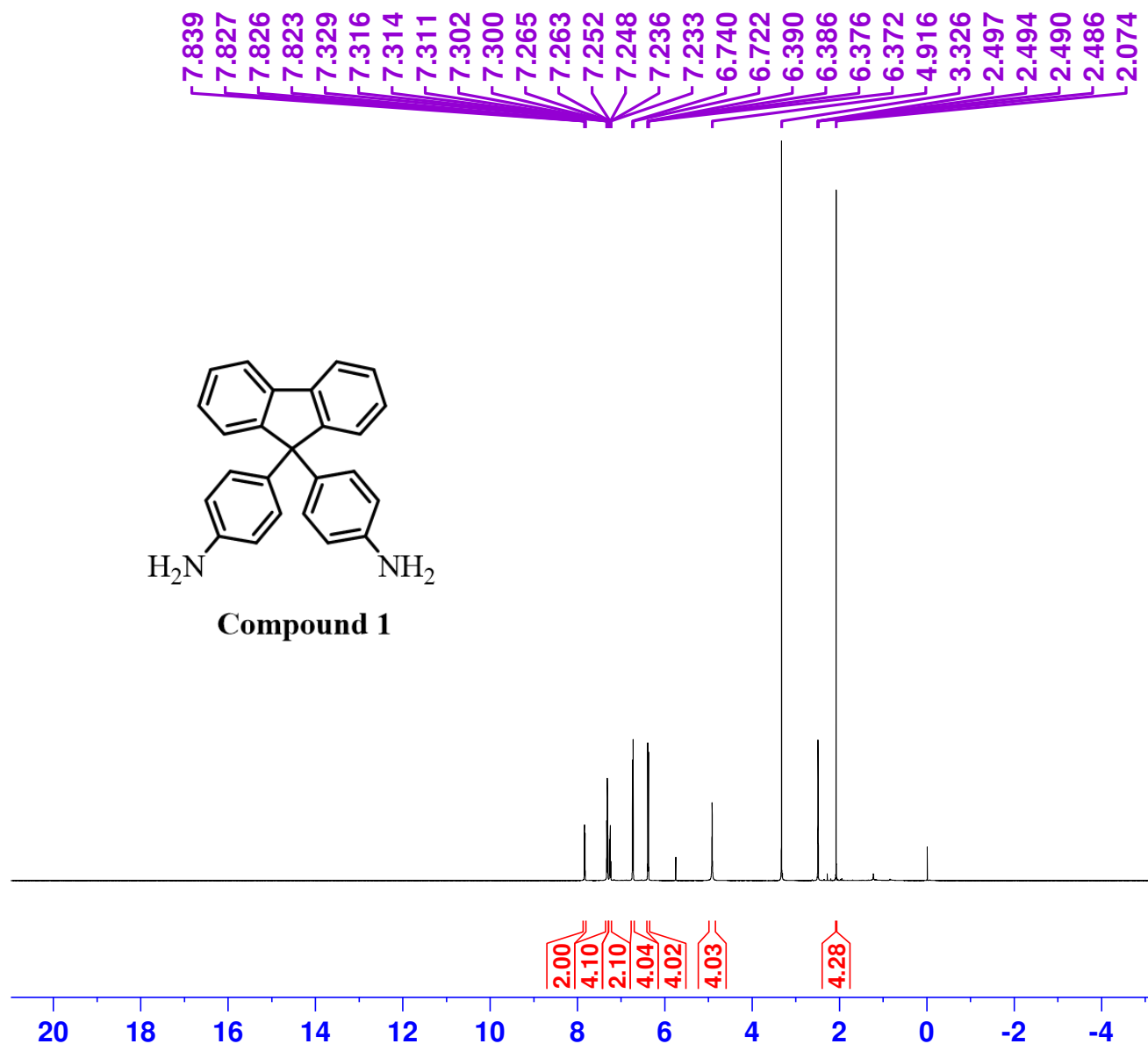


Fig. S15. The fluorescence spectra changes of probe **2** (10 μM) towards CN^- spiked industrial wastewater.

References

- 1 S. Sanjabi, J. K. Rad and A. R. Mahdavian, *J. Photochem. Photobiol. A: Chem.*, 2022, **424**, 113626.
- 2 Q. Li, J. Chang, H. Shi, T. Niu, H. Dong and H. Mu, *Supramol. Chem.*, 2022, 1-7.
- 3 L.-M. Pu, R.-Y. Li, Z.-Z. Chen, W.-B. Xu, H.-T. Long and W.-K. Dong, *J. Photochem. Photobiol. A: Chem.*, 2022, 113883.
- 4 Z. Zhang, G. Chen, W. Pan, Y. Bi, S. Shen, X. Cao, X. Pang and Y. Zhu, *J. Mol. Struct.*, 2022, **1251**, 131893.
- 5 C. Liu, D. Zhang, S. Ye, T. Chen and R. Liu, *Spectrochim. Acta A Mol. Biomol. Spectrosc.*, 2022, **267**, 120593.
- 6 R. Nazarian, H. R. Darabi, K. Aghapoor, R. Firouzi and H. Sayahi, *Chem. Comm.*, 2020, **56**, 8992-8995.
- 7 Z. M. Dong, H. Ren, J. N. Wang and Y. Wang, *Microchem. J.*, 2020, **155**, 104676.
- 8 Q. Niu, L. Lan, T. Li, Z. Guo, T. Jiang, Z. Zhao, Z. Feng and J. Xi, *Sens. Actuators B Chem.*, 2018, **276**, 13-22.
- 9 X. Wen, L. Yan and Z. Fan, *Spectrochim. Acta A Mol. Biomol. Spectrosc.*, 2020, **241**, 118664.
- 10 L. Tang, L. Zhou, A. Liu, X. Yan, K. Zhong, X. Liu, X. Gao and J. Li, *Dyes Pigm.*, 2021, **186**, 109034.

Compound 1 (1H NMR, 500 MHz, DMSO-d6)

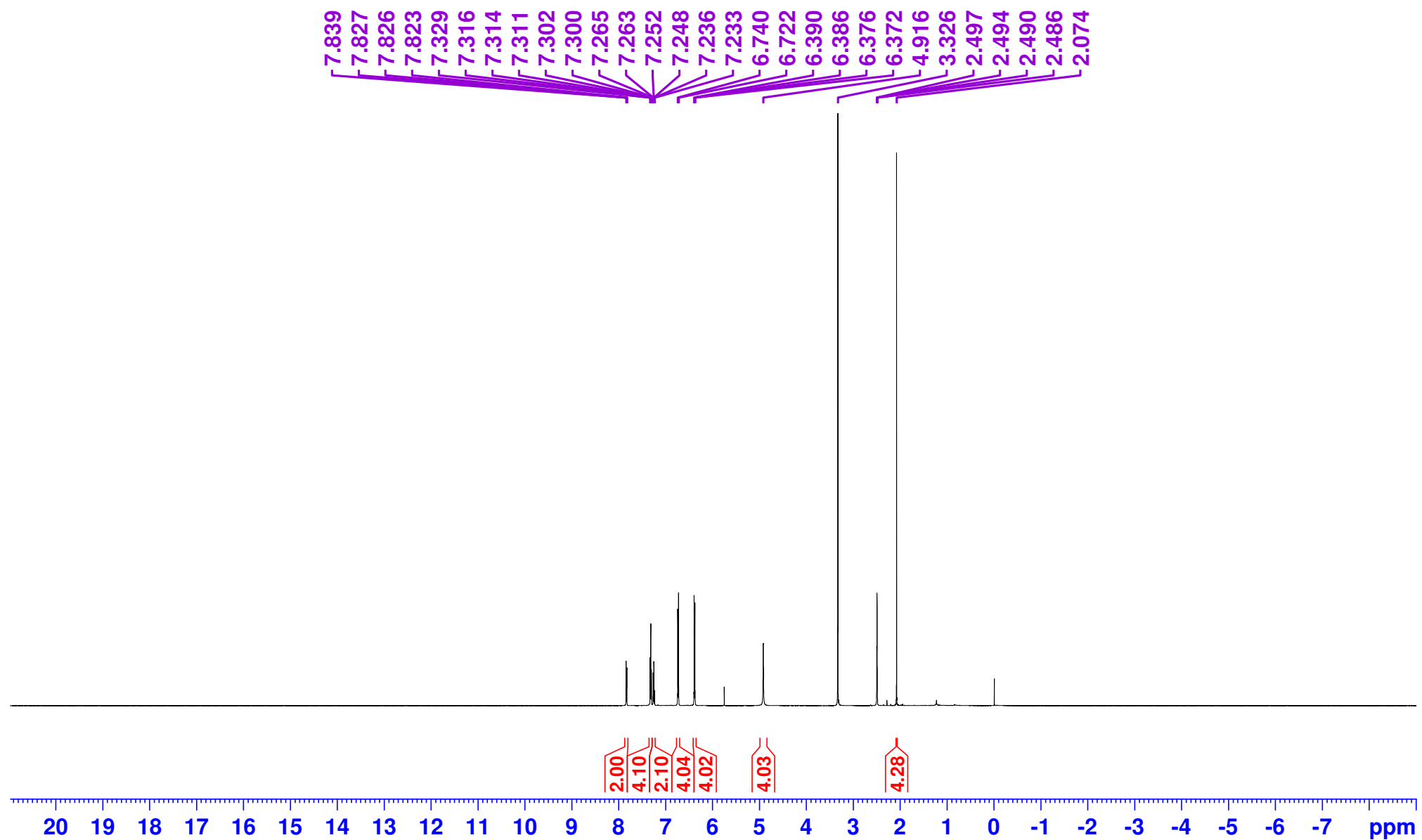


Current Data Parameters
 NAME Shumaila Majeed
 EXPNO
 PROCNO

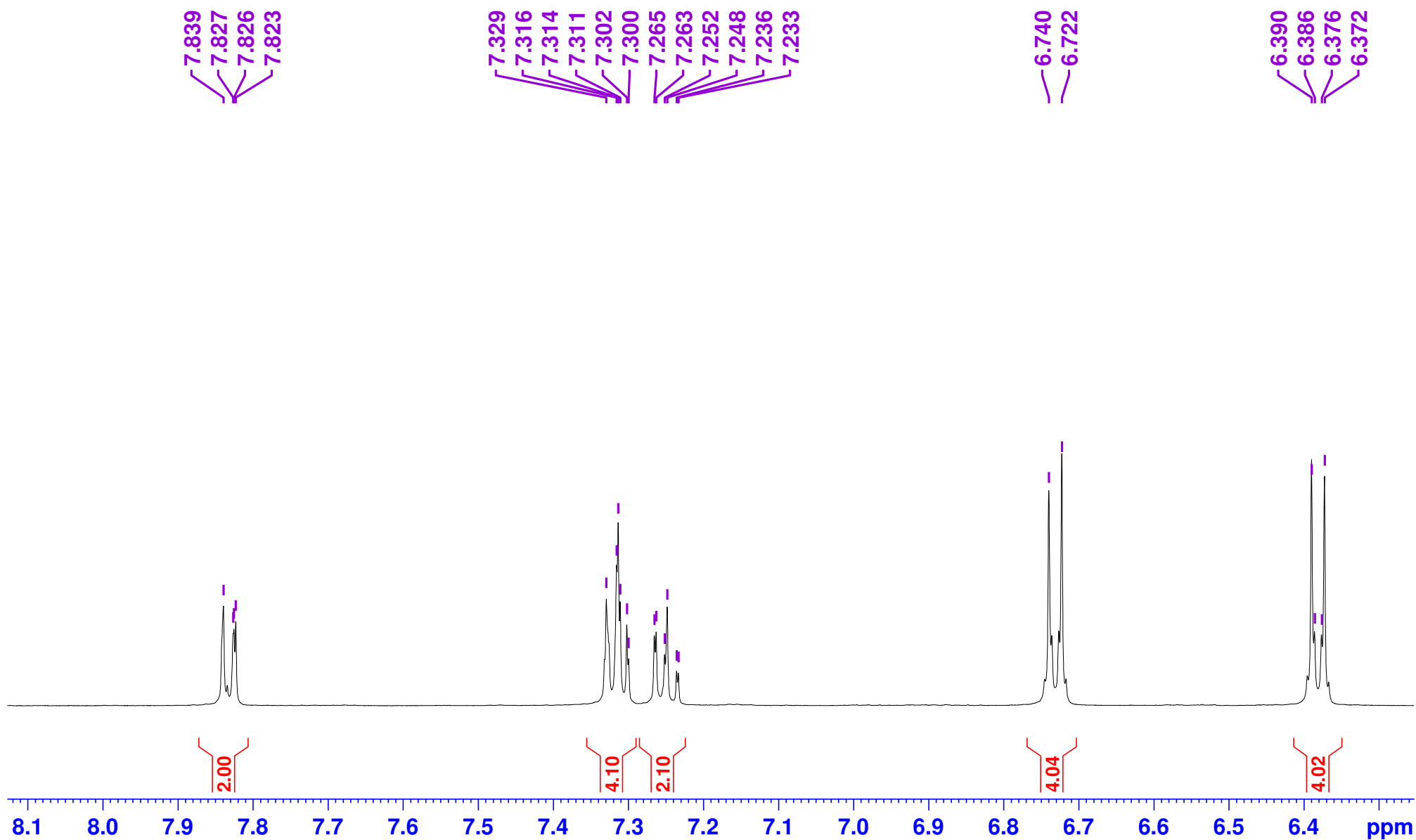
F2 - Acquisition Parameters
 Date_ 20181120
 Time 11.56 h
 INSTRUM spect
 PROBHD Z119470_0109
 PULPROG zg
 TD 65536
 SOLVENT DMSO
 NS 23
 DS 0
 SWH 15000.000 Hz
 FIDRES 0.457764 Hz
 AQ 2.1845334 sec
 RG 52.58
 DW 33.333 usec
 DE 6.50 usec
 TE 294.4 K
 D1 3.0000000 sec
 TD0 1
 SFO1 500.1830011 MHz
 NUC1 1H
 P1 11.60 usec
 PLW1 14.0000000 W

F2 - Processing parameters
 SI 131072
 SF 500.1800093 MHz
 WDW EM
 SSB 0
 LB 0.10 Hz
 GB 0
 1.00

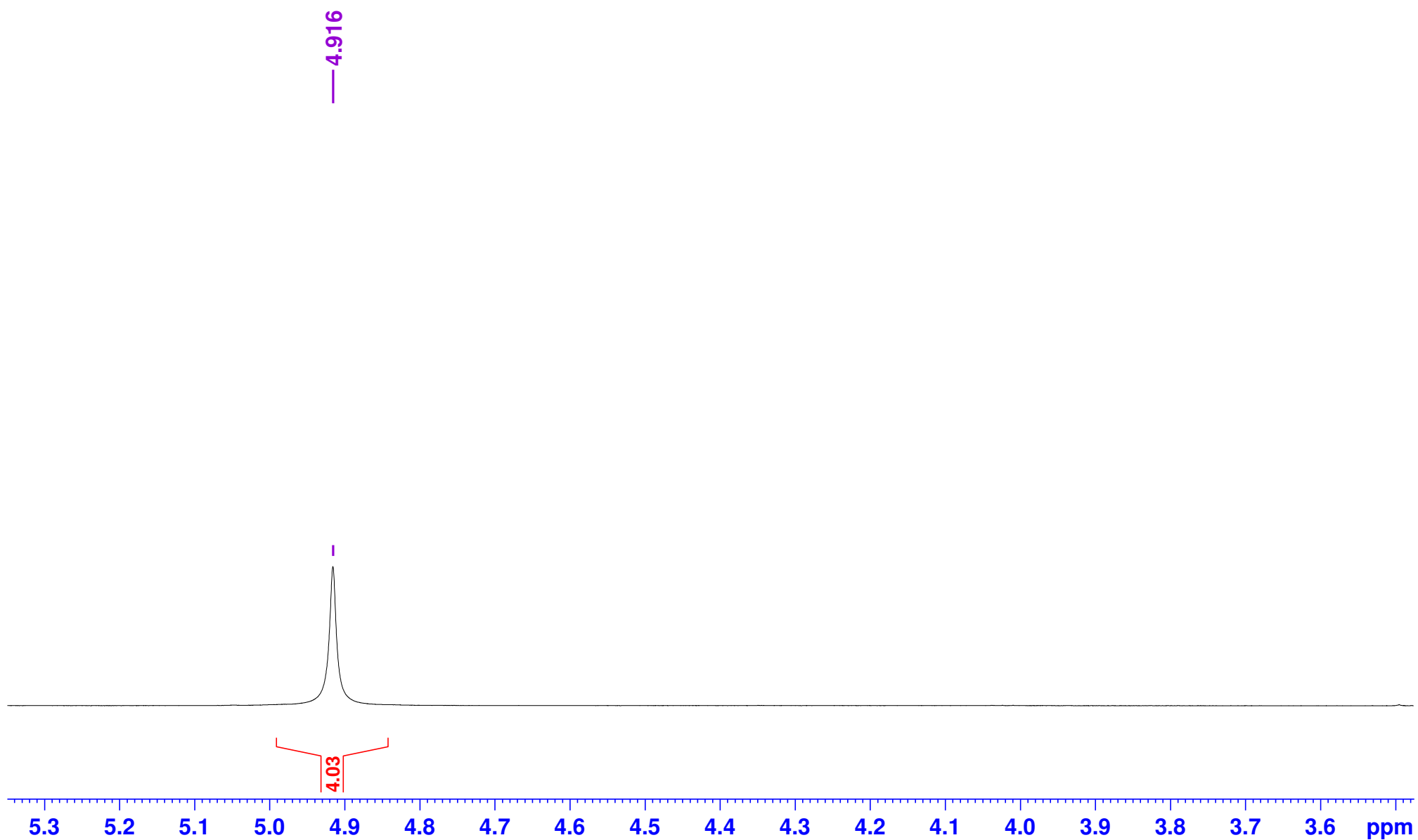
Compound 1 (1H NMR, 500 MHz, DMSO-d6)



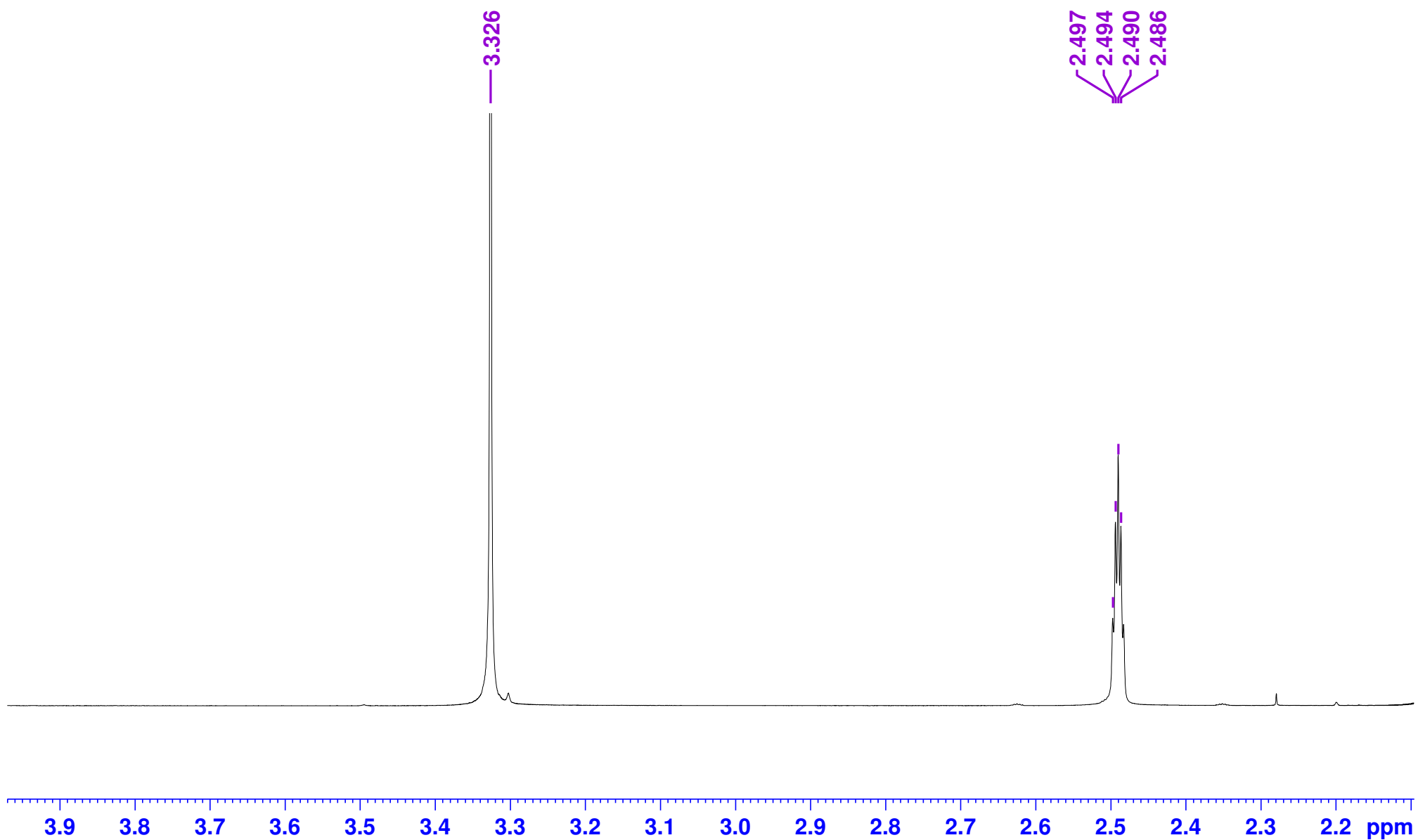
Compound 1 (1H NMR, 500 MHz, DMSO-d6)



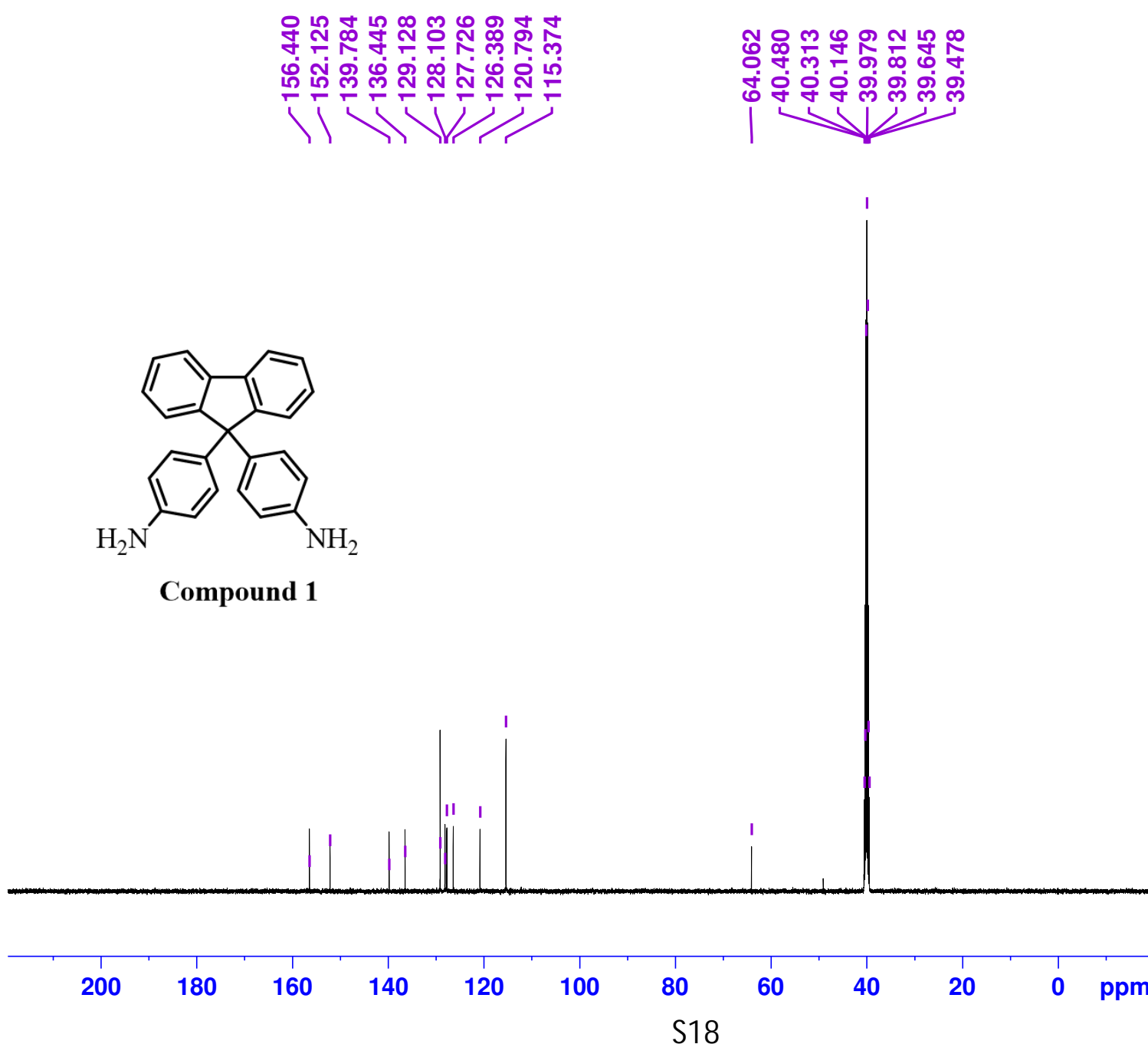
Compound 1 (1H NMR, 500 MHz, DMSO-d6)



Compound 1 (1H NMR, 500 MHz, DMSO-d6)



Compound 1 (13C NMR, 125 MHz, DMSO-d6)

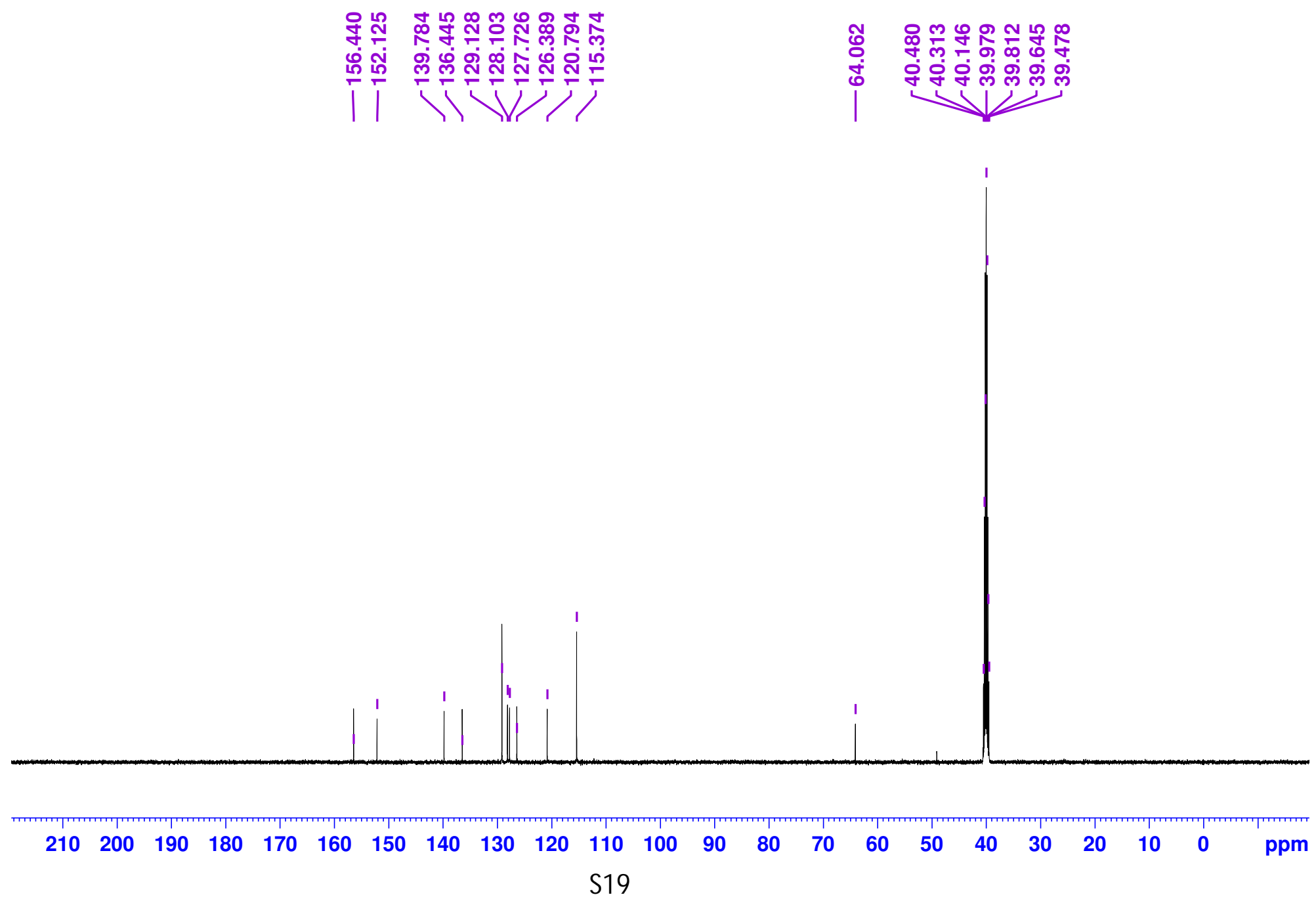


Current Data Parameters
 NAME Shumaila Maj
 EXPNO
 PROCNO

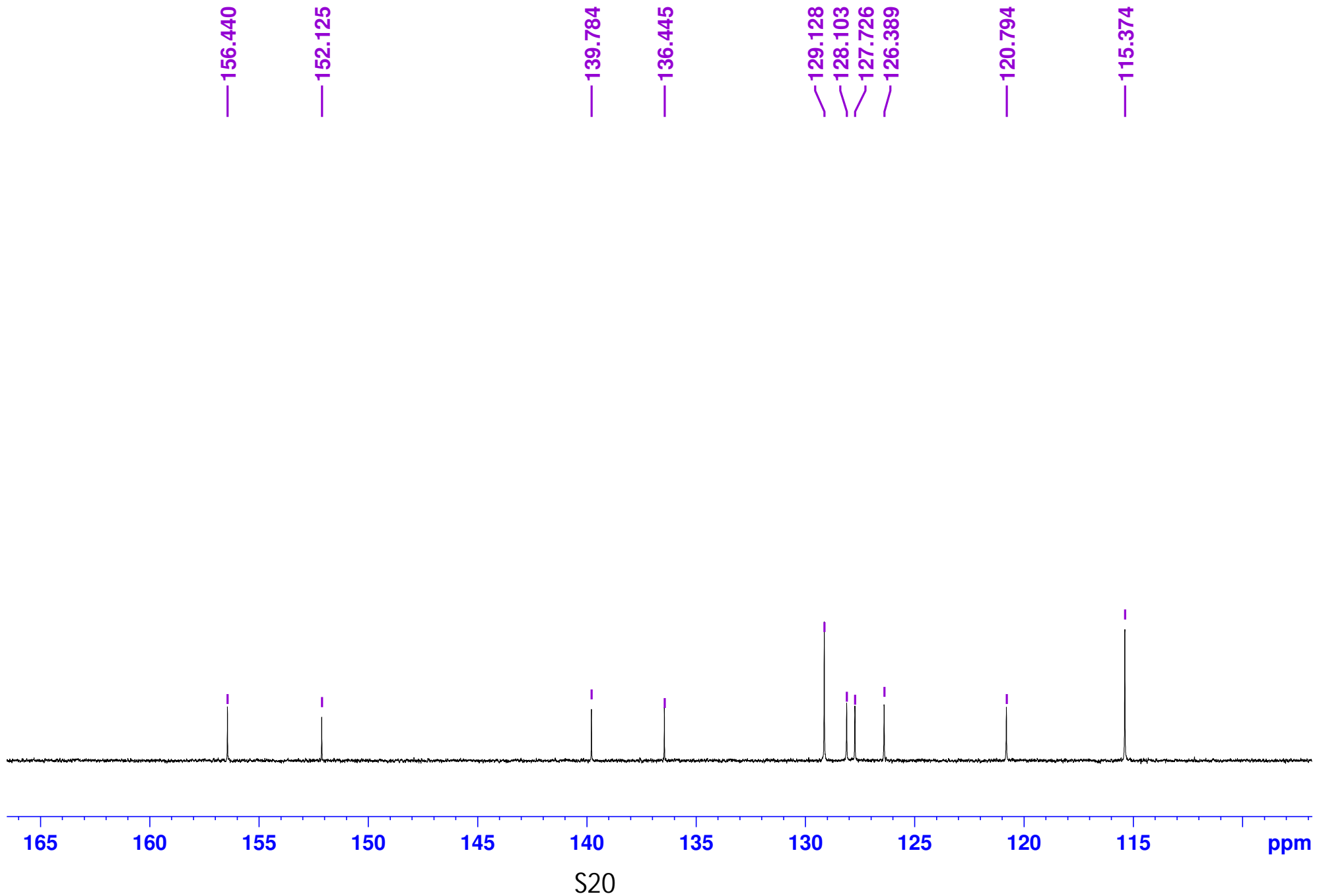
F2 - Acquisition Parameters
 Date_ 20190122
 Time 7.02 h
 INSTRUM spect
 PROBHD Z119470_0109
 PULPROG zgdc30
 TD 65536
 SOLVENT DMSO
 NS 300
 DS 0
 SWH 37878.789 Hz
 FIDRES 1.155969 Hz
 AQ 0.8650752 sec
 RG 188.37
 DW 13.200 usec
 DE 6.50 usec
 TE 294.5 K
 D1 2.00000000 sec
 D11 0.03000000 sec
 TDO 1
 SFO1 125.7829380 MHz
 NUC1 13C
 P0 3.10 usec
 P1 9.30 usec
 PLW1 80.0000000 W
 SFO2 500.1820007 MHz
 NUC2 1H
 CPDPRG[2] waltz16
 PCPD2 80.00 usec
 PLW2 14.00000000 W
 PLW12 0.29435000 W

F2 - Processing parameters
 SI 131072
 SF 125.7703616 MHz
 WDW EM
 SSB 0
 LB 1.00 Hz
 GB 0
 PC 1.40

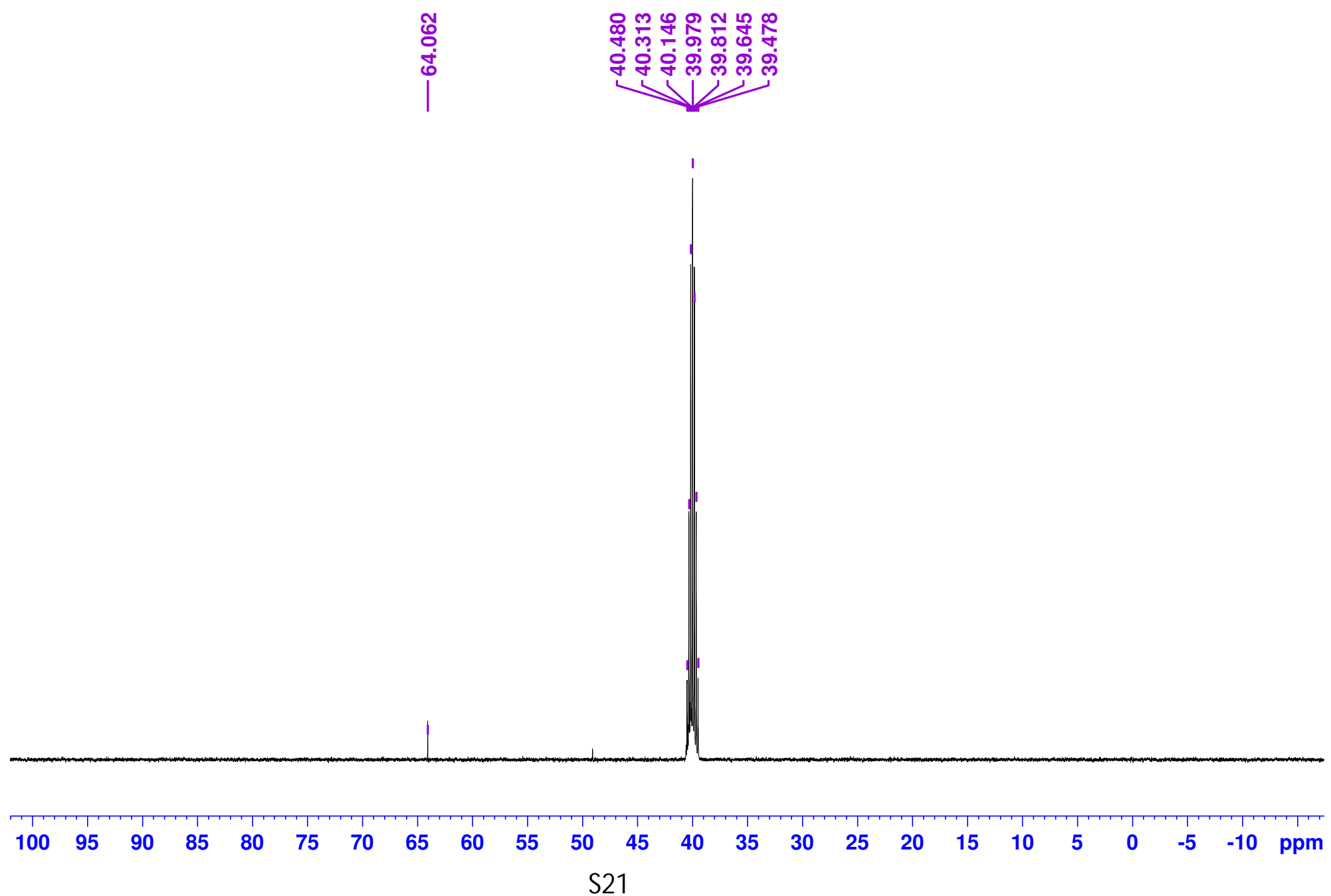
Compound 1 (¹³C NMR, 125 MHz, DMSO-d₆)



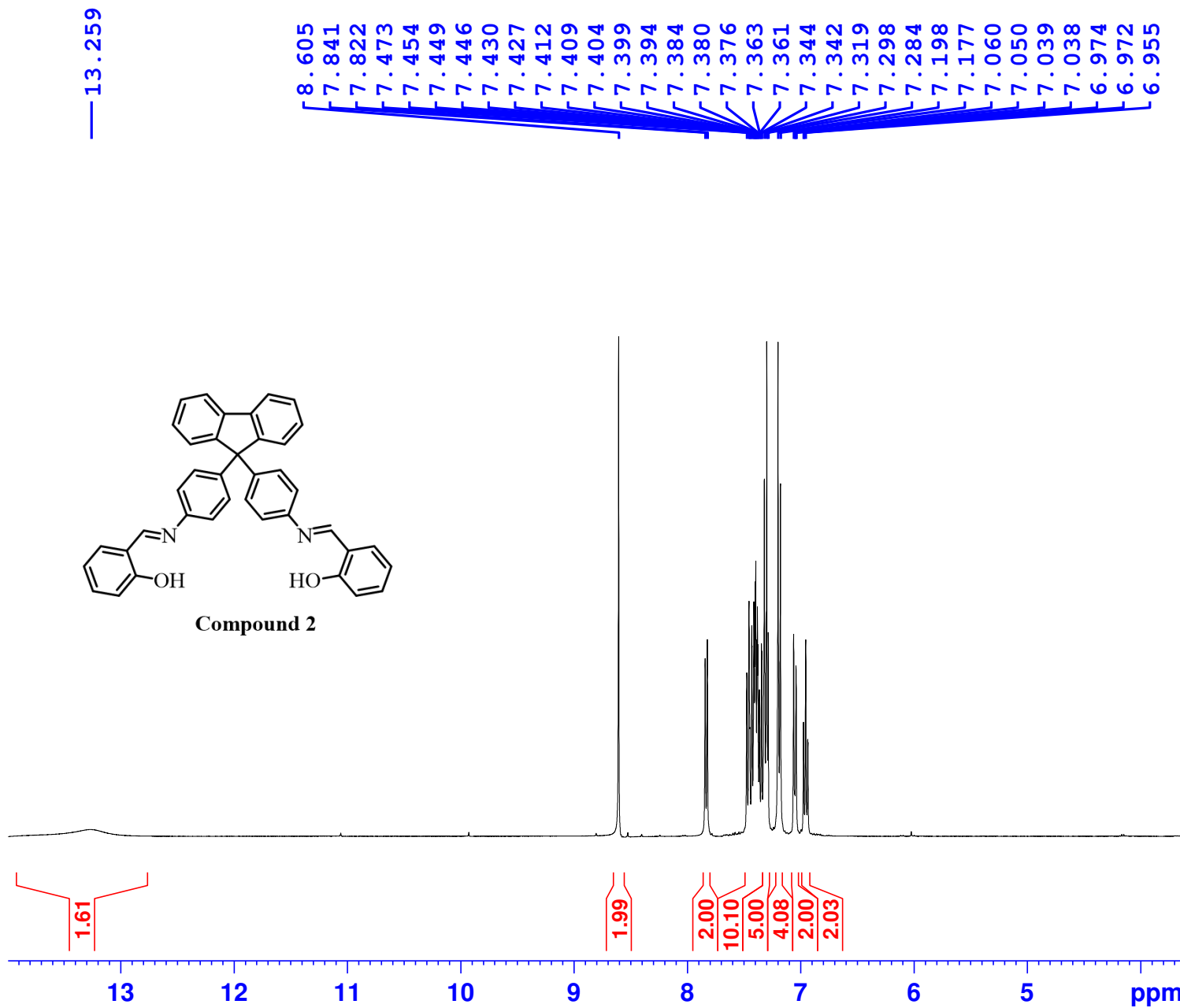
Compound 1 (^{13}C NMR, 125 MHz, DMSO-d₆)



Compound 1 (^{13}C NMR, 125 MHz, DMSO-d₆)



Compound 2 (1H NMR, 400 MHz, CDCl₃)





Current Data Parameters
NAME Shumaila Majeed
EXPNO
PROCNO

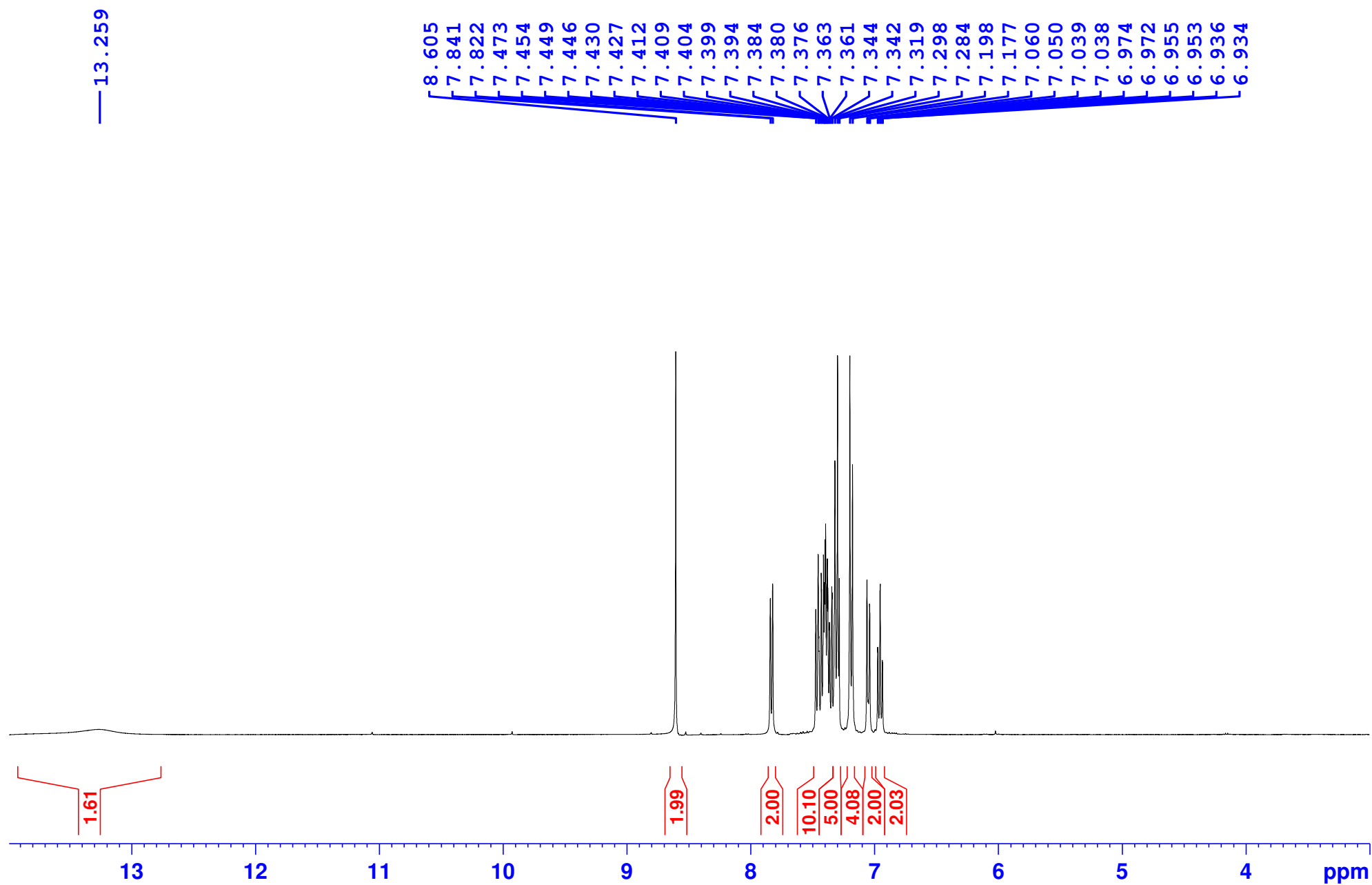
```

F2 - Acquisition Parameters
Date_           20190718
Time            16.33 h
INSTRUM        spect
PROBHD         Z116098_0621
PULPROG        zg30
TD              65536
SOLVENT         CDC13
NS              16
DS              2
SWH             5597.015 Hz
FIDRES         0.170807 Hz
AQ              5.8545494 sec
RG              78.01
DW              89.333 usec
DE              6.50 usec
TE              298.0 K
D1              1.00000000 sec
TD0                 1
SFO1          400.1328009 MHz
NUC1            1H
P1              10.00 usec
P1W1           16.68099976 w

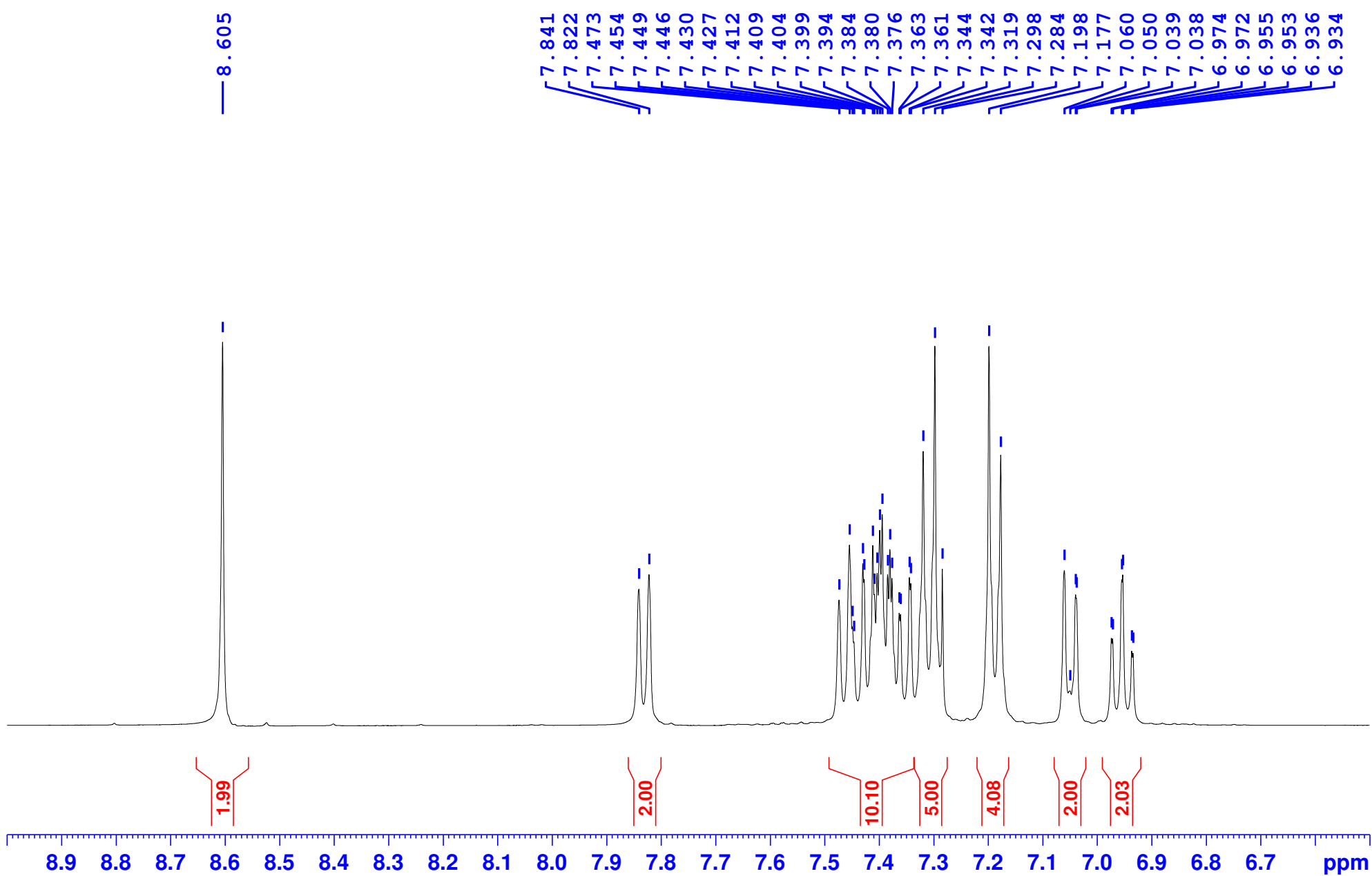
```

F2 - Processing parameters
SI 65536
SF 400.1300000 MHz
WDW EM
SSB 0
LB 0.30 Hz
GB 0
PC 1.00

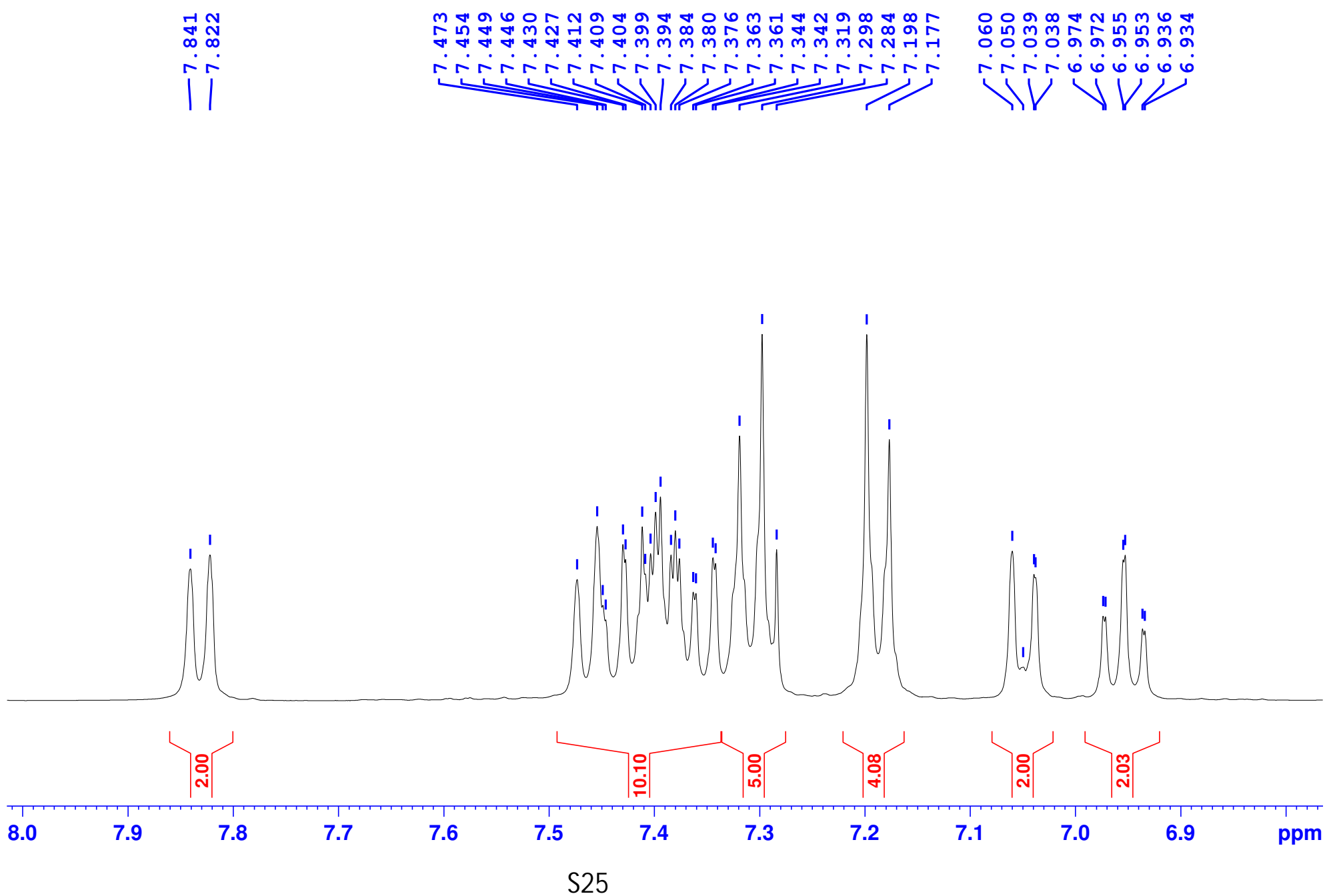
Compound 2 (1H NMR, 400 MHz, CDCl₃)



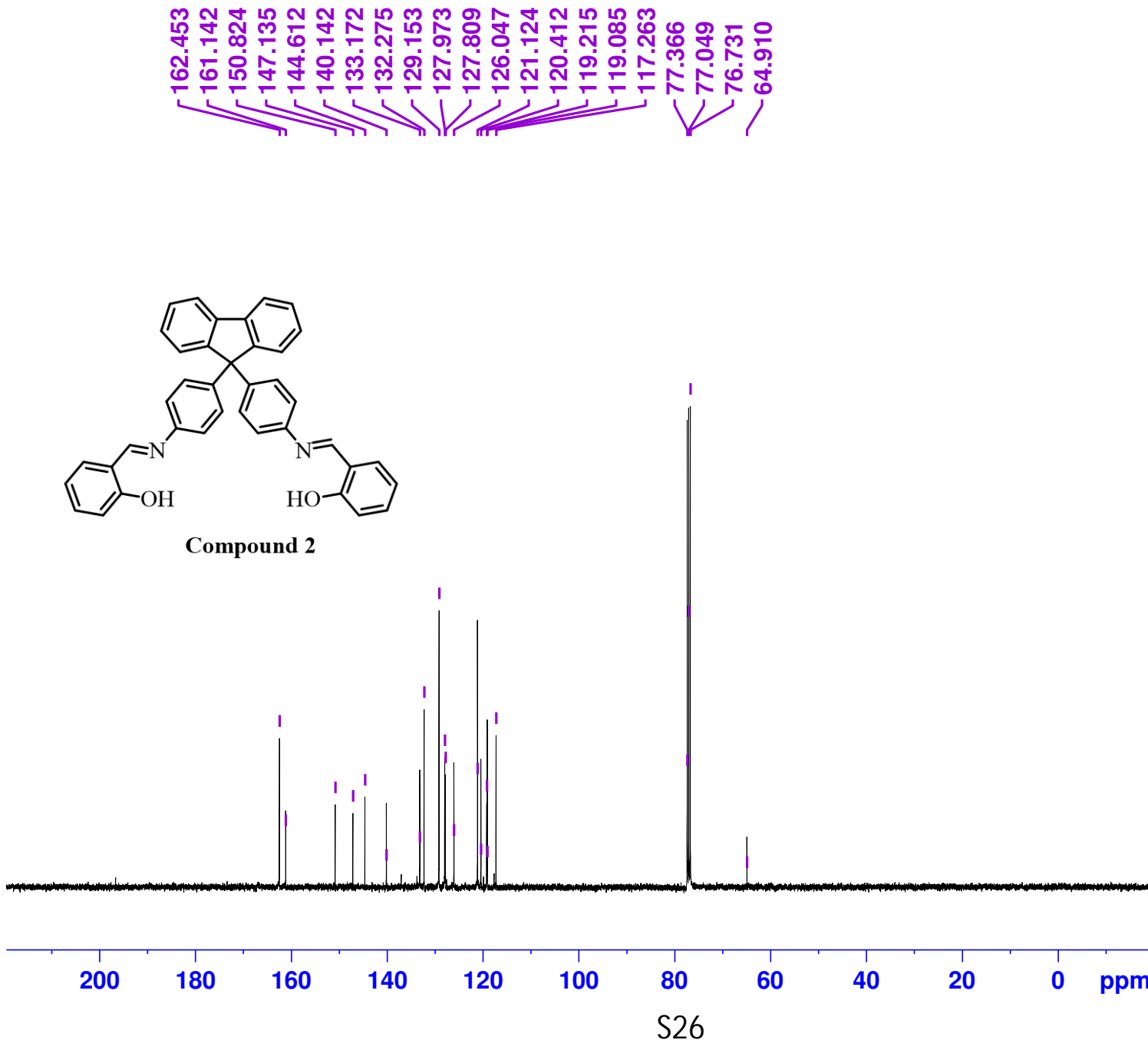
Compound 2 (1H NMR, 400 MHz, CDCl₃)



Compound 2 (1H NMR, 400 MHz, CDCl₃)



Compound 2 (13C NMR, 400 MHz, CDCl₃)

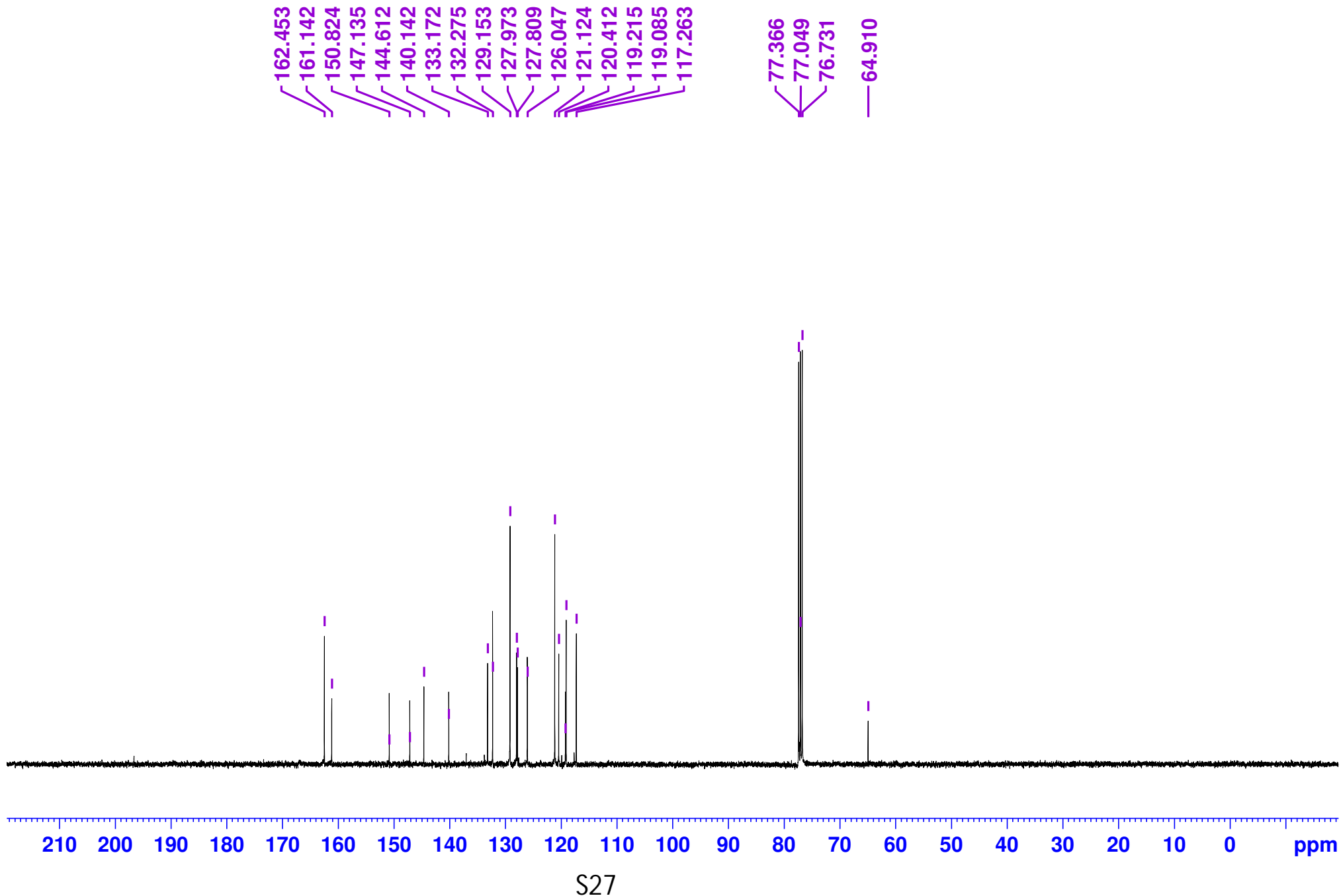


Current Data Parameters
 NAME Shumaila Majeed
 EXPNO
 PROCNO

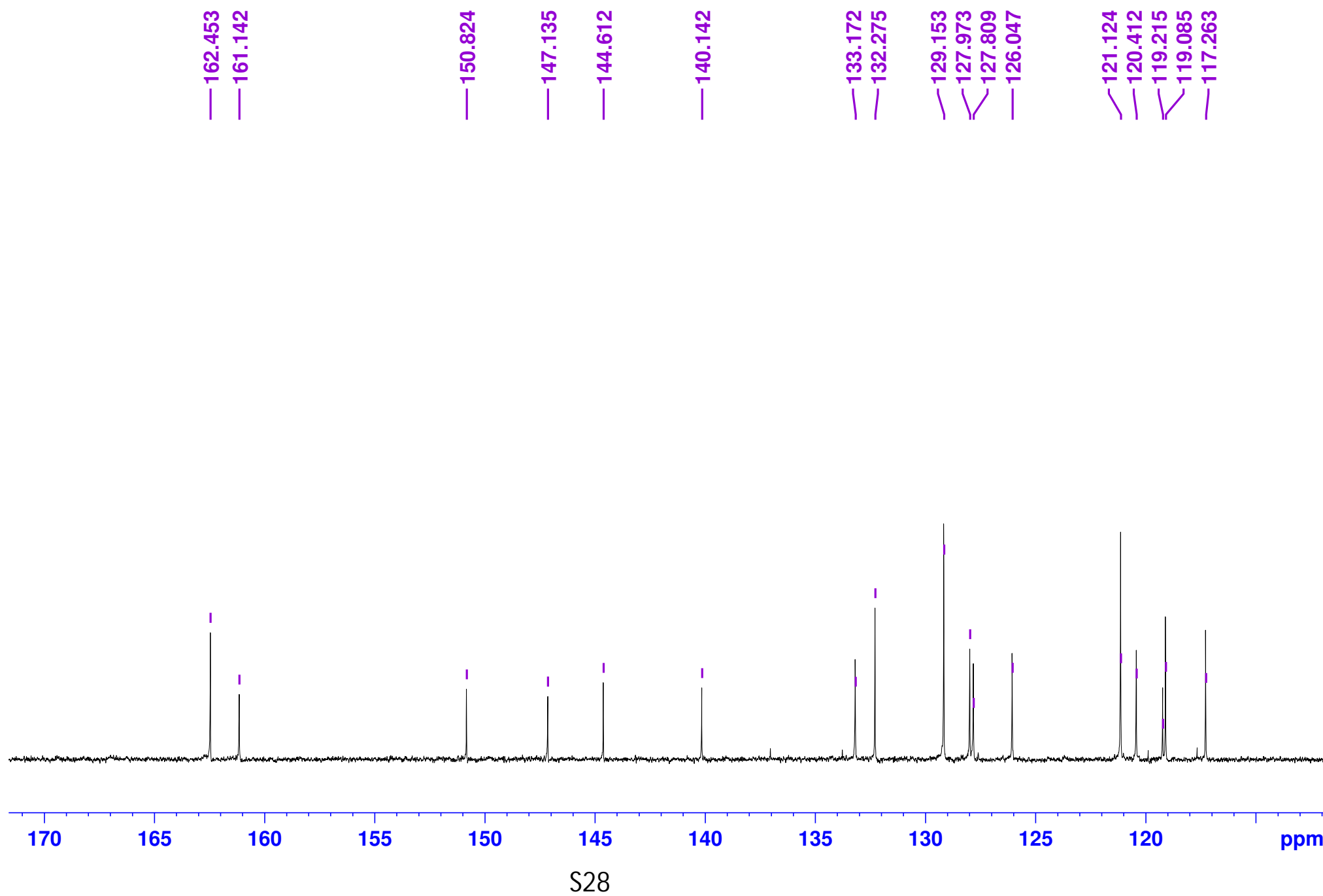
F2 - Acquisition Parameters
 Date_ 20190719
 Time 15.53 h
 INSTRUM spect
 PROBHD Z116098_0621
 PULPROG zgpg30
 TD 65536
 SOLVENT CDCl₃
 NS 400
 DS 4
 SWH 24038.461 Hz
 FIDRES 0.733596 Hz
 AQ 1.3631488 sec
 RG 199.48
 DW 20.800 usec
 DE 6.50 usec
 TE 298.0 K
 D1 2.0000000 sec
 D11 0.03000000 sec
 TDO 1
 SFO1 100.6228298 MHz
 NUC1 ¹³C
 P1 10.00 usec
 PLW1 72.56700134 W
 SFO2 400.1316005 MHz
 NUC2 ¹H
 CPDPRG[2] waltz16
 PCPD2 90.00 usec
 PLW2 16.68099976 W
 PLW12 0.20593999 W
 PLW13 0.10342000 W

F2 - Processing parameters
 SI 32768
 SF 100.6127685 MHz
 WDW EM
 SSB 0
 LB 1.00 Hz
 GB 0
 PC 1.40

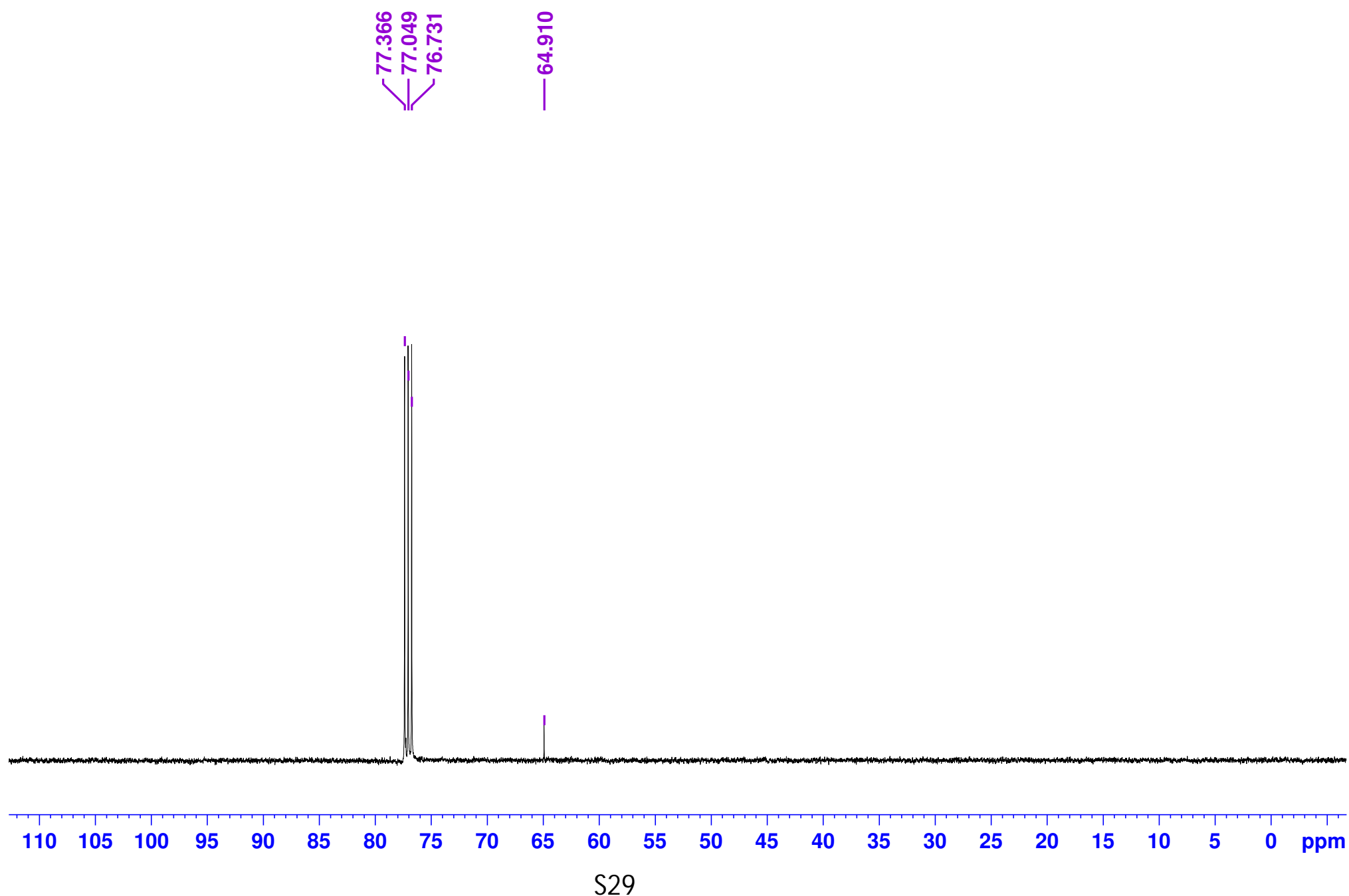
Compound 2 (^{13}C NMR, 400 MHz, CDCl_3)



Compound 2 (13C NMR, 400 MHz, CDCl3)



Compound 2 (13C NMR, 400 MHz, CDCl₃)



Compound 2 (Mass spectrum)

SMSB_220513095820 #1 RT: 0.00 AV: 1 NL: 2.22E5
T: ITMS + p ESI Full ms [50.00-1500.00]

